

## A Damaging Downburst Prediction and Detection Algorithm for the WSR-88D

TRAVIS M. SMITH,\* KIMBERLY L. ELMORE,\* AND SHANNON A. DULIN\*

*Cooperative Institute for Mesoscale Meteorological Studies, University of Oklahoma, Norman, Oklahoma*

(Manuscript received 10 September 2002, in final form 20 August 2003)

### ABSTRACT

The problem of predicting the onset of damaging downburst winds from high-reflectivity storm cells that develop in an environment of weak vertical shear with Weather Surveillance Radar-1988 Doppler (WSR-88D) is examined. Ninety-one storm cells that produced damaging outflows are analyzed with data from the WSR-88D network, along with 1247 nonsevere storm cells that developed in the same environments. Twenty-six reflectivity and radial velocity-based parameters are calculated for each cell, and a linear discriminant analysis was performed on 65% of the dataset in order to develop prediction equations that would discriminate between severe downburst-producing cells and cells that did not produce a strong outflow. These prediction equations are evaluated on the remaining 35% of the dataset. The datasets were resampled 100 times to determine the range of possible results. The resulting automated algorithm has a median Heidke skill score (HSS) of 0.40 in the 20–45-km range with a median lead time of 5.5 min, and a median HSS of 0.17 in the 45–80-km range with a median lead time of 0 min. As these lead times are medians of the mean lead times calculated from a large, resampled dataset, many of the storm cells in the dataset had longer lead times than the reported median lead times.

### 1. Introduction

Predicting the onset of severe wind events is a difficult challenge for weather forecasters. Although a large percentage of severe wind reports that are logged in the United States can be attributed to dynamically driven derechos from mesoscale convective systems (Johns and Hirt 1987) or high-precipitation supercells, some regions of the United States, most frequently the Southeast and desert Southwest, experience numerous summertime severe wind events from single cells or multi-cell clusters that tend to form in regions of moderate-to-high convective available potential energy (CAPE), weak environmental shear, and environments that are highly unstable to downdrafts. These downbursts—strong downdrafts that induce strong outflows at the surface (Fujita 1981)—originate from storm cells that typically have life cycles on the order of 20 to 40 min and a horizontal scale less than 10 km, as opposed to longer-lived derecho events produced by convective lines that have life cycles on the order of many hours and a horizontal scale of several hundred kilometers (Johns and Hirt 1987). This makes severe outflows from these “pulse” thun-

derstorms difficult for weather forecasters to issue warnings for as well as being a danger to aviators.

The installation of the Weather Surveillance Radar-1988 Doppler (WSR-88D) units that make up the Next-Generation Weather Radar (NEXRAD) network (Klazura and Imy 1993; Crum and Alberty 1993) has provided forecasters with abundant storm-scale meteorological data. Forecasters frequently use computer algorithms as guidance to help identify important storm features that might otherwise be difficult to detect in this wealth of information. Additionally, these algorithms extract quantitative data characteristics of radar-sampled phenomena instead of only qualitative characteristics of a data field. For instance, the Storm Cell Identification and Tracking (SCIT) algorithm (Johnson et al. 1998), the Tornado Detection Algorithm (TDA; Mitchell et al. 1998), the Mesocyclone Detection Algorithm (MDA; Stumpf et al. 1998), and the Hail Detection Algorithm (HDA; Witt et al. 1998) are quantitative warning guidance tools that have been developed to assist forecasters who may be overwhelmed by these large amounts of data. However, no radar warning guidance for damaging wind events that are hazardous to both aviators and the public exists in the current WSR-88D system. Therefore, we have designed the Damaging Downburst Prediction and Detection Algorithm (DDPDA) to assist forecasters who are tasked with issuing warnings for these events. The DDPDA predicts and detects very strong outflows from storms that develop in an environment of weak vertical wind shear,

\* Additional affiliation: National Severe Storms Laboratory, Norman, Oklahoma.

Corresponding author address: Travis M. Smith, NOAA/NSSL, 1313 Halley Circle, Norman, OK 73069.  
E-mail: Travis.Smith@noaa.gov

where the surface-to-500-mb wind shear ranges from 0 to 15 m s<sup>-1</sup>.

Whereas earlier studies have typically examined downburst events that were well sampled with one or more high-resolution Doppler radars (Mahoney and Elmore 1991; Roberts and Wilson 1989; Atkins and Wakimoto 1991), this study focuses on the statistical properties of downburst-producing cells that are observed with WSR-88Ds that have a beamwidth of 0.95° and gate spacing of 250 m in range. Wolfson et al. (1994) describe a microburst prediction algorithm that attempts to address the same forecasting challenge near large airports by ingesting data from the Federal Aviation Administration's (FAA) higher-resolution Terminal Doppler Weather Radar (TDWR), which has finer horizontal, vertical, and temporal resolution than the WSR-88D. The Wolfson et al. algorithm uses two-dimensional image-processing techniques that track a combination of cell growth features [increasing vertically integrated liquid (VIL) and vertically integrated frozen water], decay features (descending center of mass and echo bottom), and preexisting outflows, and then issues downburst predictions for outflow strengths that exceed 15.4 m s<sup>-1</sup> (30 kt). In contrast, the DDPDA uses up to 26 WSR-88D cell-based algorithmic parameters, described in section 2b, as input into its analysis and issues downburst predictions for the National Weather Service's severe convective wind criteria as described in section 2a.

In an analysis of 31 cells in Colorado, Roberts and Wilson (1989) identified a number of radar signatures that preceded the occurrence of microburst events. These precursors included descending reflectivity cores, reflectivity notches, radial convergence within the cloud, and rotation. Similarly, Eilts et al. (1996a) examined 85 damaging downbursts from many different environmental regimes to determine what precursors were most important in these intense events. The three most significant precursors Eilts et al. found in this dataset included a rapidly descending reflectivity core, strong and deep convergence at midaltitudes (2–6 km above ground level), and a reflectivity core that initially begins at a height higher than most other storms. Here, we examine variations on these parameters to determine how they might be used to predict strong outflows with WSR-88Ds.

Our methodology is to (a) gather a dataset of severe wind events, (b) calculate parameters that may be related to the onset of strong outflows at the surface, (c) use a linear discriminant analysis to develop equations that discriminate between severe and nonsevere outflows, and (d) verify the results on an independent dataset. This paper is divided into the following sections:

- section 2 provides a discussion of the methodology for collecting the data and devising a process to discriminate between severe and nonsevere storm cells,
- section 3 contains an evaluation of these results,

- section 4 contains a functional description of the DDPDA, and
- section 5 provides a discussion of the practical uses of the DDPDA as well as its limitations.

## 2. Method

### a. Dataset

Obtaining reliable data that can be used to develop and evaluate forecast algorithms is always problematic. The DDPDA uses storm reports from the National Climatic Data Center's *Storm Data* publication supplemented with low-altitude radial divergence signatures in radar data. The reports are carefully matched to a divergence signature in the radial velocity field. Frequently, if the storm report was from a spotter, the report time lags the initial divergence signature by several minutes to an hour. However, anemometer reports of maximum gusts are always a much better time match. The final dataset consists of radar-detected storm cells that can be classified as producing "severe" or "nonsevere" outflows near the surface beginning at a specific time. Because radar resolution degrades as range increases, all cells in the database are within 80 km of a WSR-88D. Finally, because the DDPDA is designed to detect and predict downburst events that occur in a moderate-to-high CAPE and low-shear (surface-to-500-mb wind shear of 0 to 15 m s<sup>-1</sup>) environment, all the cases in the database must adhere to this standard as well. Low-reflectivity downbursts are excluded from the database because of the small sample size of validation data for such events.

We define a "severe" cell by one or more of the following criteria:

- produced a measured wind gust of 50 kt (about 26 m s<sup>-1</sup>) at the surface
- produced damage that was recorded in *Storm Data* or in National Weather Service storm spotter logs
- produced a radar-measured wind of 25 m s<sup>-1</sup> or a divergence signature with a radial velocity difference exceeding 40 m s<sup>-1</sup> within 1 km of the surface

Most *Storm Data* reports must be altered to correct erroneous times. Additionally, although the radar-based criteria are a proxy for surface wind measurements, we believe that these cells produced "severe" outflow at the surface. Hjelmfelt (1988) has shown that single-Doppler estimates of maximum velocity differentials frequently underestimate the true differential by 50% or greater. These standards also exceed the downburst criteria used by the Federal Aviation Administration to assess hazards to aircraft (Federal Aviation Administration 1987), which is one focus of the DDPDA.

In order to define "nonsevere" cells for the database, it is necessary to include only those cells that we are confident did not produce a strong, damaging outflow. Since many strong cells occur over areas with low pop-



TABLE 2. The integrated parameters imported or calculated by the DDPA. The variable name is listed, followed by the type of data the parameter is derived from (*R* is reflectivity, *V* is radial velocity, and *E* is environmental) and a description of how it is calculated.

Variable name	Type	Description
VIL	<i>R</i>	Cell-based VIL
MASSHT	<i>R</i>	Height of the center of mass
VOL	<i>R</i>	Cell volume
ASP	<i>R</i>	Core aspect ratio (ratio of cell depth to cell width)
SHI	<i>R</i>	Severe hail index (Witt et al. 1998)
MAXDBZ	<i>R</i>	Max reflectivity
DBZHT	<i>R</i>	Height of the max reflectivity
DBZ7KM	<i>R</i>	Max reflectivity above 7 km MSL
ZTHTE	<i>R/E</i>	Max reflectivity near the height of the min environmental $\theta_e$
ZATHTE	<i>R/E</i>	Max reflectivity above the height of the min environmental $\theta_e$
CNVMELT	<i>V/E</i>	Max linear LS convergence* near the height of the environmental 0°C isotherm
CTHTE	<i>V/E</i>	Max LS convergence* near the height of the min environmental $\theta_e$
C16	<i>V</i>	Max LS convergence* in the 1–6-km-MSL layer
DVMELT	<i>V/E</i>	Max convergent $\Delta V$ near the height of the environmental 0°C isotherm
DVTHTE	<i>V/E</i>	Max convergent $\Delta V$ near the height of the min environmental $\theta_e$
DV16	<i>V</i>	Max convergent $\Delta V$ in the 1–6-km-MSL layer
DPTHV	<i>V</i>	Depth of LS convergence* exceeding 0.004 s <sup>-1</sup>
DPTHDV	<i>V</i>	Depth of convergent $\Delta V$ exceeding 10 m s <sup>-1</sup>
MAXR17	<i>V</i>	Max positive rotation in the 1–7-km-MSL layer
MINR17	<i>V</i>	Min negative rotation in the 1–7-km-MSL layer
CMEAN16	<i>V</i>	Mean LS convergence* in the 1–6-km-MSL layer
DV3	<i>V</i>	Max convergent $\Delta V$ in the 1–6 km MSL layer, min/max can be separated by up to 3 radials
CONV006	<i>V</i>	The cross-sectional area coverage of convergence* in the 1–6-km-MSL layer that exceeds 0.006 s <sup>-1</sup>
CONV004	<i>V</i>	The cross-sectional area coverage of convergence* in the 1–6-km-MSL layer that exceeds 0.004 s <sup>-1</sup>
CONV002	<i>V</i>	The cross-sectional area coverage of convergence* in the 1–6-km-MSL layer that exceeds 0.002 s <sup>-1</sup>
CONV001	<i>V</i>	The cross-sectional area coverage of convergence* in the 1–6-km-MSL layer that exceeds 0.001 s <sup>-1</sup>

\* “Convergence” refers to radial velocity estimates of convergence.

median filter to remove outlying values. The divergent portion of the shear,  $u_r$ , is calculated via the equation

$$u_r = \frac{\sum i u_{ij}}{50\Delta r},$$

while the rotational portion,  $u_s$ , is given by

$$u_s = \frac{\sum j u_{ij}}{50r_0\Delta\phi},$$

where (*i, j*) specify the position from the center of the 5 × 5 matrix (−2, −1, 0, 1, 2),  $\Delta r$  is the gate spacing,  $\Delta\phi$  is the beamwidth in meters (and, hence, a function of range),  $u_{ij}$  is the radial velocity at each point, and  $r_0$  is the range.

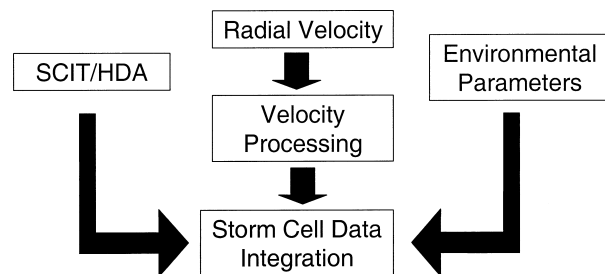


FIG. 2. The data assimilation process used to gather information on each storm cell.

*c. Analysis of parameters for downburst prediction*

To develop predictive classification equations, storm cells are randomly classified into either a “training” (dependent) or “validation” (independent) dataset. Hence, each cell has a 65% chance of being grouped into the training dataset and a 35% chance of being grouped into the validation dataset. This process is repeated 100 times so that the variability of the skill scores might be assessed. Thus, there are 100 training datasets and 100 accompanying validation datasets for use in the development of downburst prediction equations.

Each of the 100 training datasets is separated into two parts. The first group, called the downburst-producing volume scans, consists of the four volume scans prior to and including the event time for downburst-producing cells. The second, much larger group, called the non-severe volume scans, consists of all of the volume scans of all cells that did not produce severe downburst events.

Linear discriminant analysis, described by Wilks (1995) and Huberty (1994), among others, was used to develop a set of downburst prediction equations on the training datasets. Linear discriminant analysis is a useful tool for classifying multivariate datasets into two or more groups—in this case, severe downburst-producing cells versus nonsevere cells. The forward stepwise method of discriminant analysis is employed so that the most relevant nonredundant variables would be included in the prediction equations (Huberty 1994). As different

variables have value in the identification of downburst events depending on the range from the radar, separate prediction, or classification, equations are developed for the range bands of 20–45 and 45–80 km from the radar. Since the middle and upper altitudes of storms are not sampled at close ranges to WSR-88Ds, no prediction equations are developed for cells at ranges closer than 20 km. The specific equations used in the DDPDA are described in section 3.

#### d. Detection of downburst outflows

The DDPDA includes a routine that detects divergence signatures at low altitudes and flags them as a “downburst detection” if they meet certain criteria. These routines do not provide input into the “downburst prediction” process described in section 2c but are treated separately because they do not provide any predictive capability. First, consecutive gates of  $u_r$  exceeding a threshold (default of  $0.0008 \text{ s}^{-1}$ ) are identified along a radial. These “segments” of divergence must meet a minimum length threshold (default of 1.5 km) and must be within a certain radius (default of 5 km) of a storm centroid produced by the SCIT algorithm. The maximum radial velocity difference ( $\Delta V$ ) and absolute radial wind speed (ARWS) are computed for all segments and stored for each storm cell identified by the SCIT algorithm. Divergence signatures may be sampled at any radar elevation scan with a beam centerline lower than a certain height (default of 1 km) above the elevation of the radar pedestal.

A downburst detection alert is issued if the criteria described in section 2a are met ( $\text{ARWS} \geq 25 \text{ m s}^{-1}$  or  $\Delta V \geq 40 \text{ m s}^{-1}$ ). Lesser criteria may also be used to detect weaker signatures. These signatures are usually only observed in fairly close proximity to a radar, and how well sampled they are depends on outflow depth. While the prediction functions of the DDPDA are evaluated against a combination of wind observations, damage reports, and radar-detected outflows, the detection functions of the algorithm may only be evaluated against wind observations and damage reports. For 33 damage reports within 45 km of the radar, 11 had associated downburst signatures that met the severe criteria, with the performance within 25 km being much better than at the longer ranges. Divergence signatures were detected with the other 22 events, but these radial velocity signatures did not exceed the thresholds for a severe detection alert to be issued. Because of the limitations of the verification data, it is not possible to determine if false warnings are issued. Although it is likely that lower thresholds will allow for an increased probability of detection, the sample size of potentially well-sampled outflows and surface verification data is too small for reliable results.

#### e. Scoring method

The scoring methodology used to evaluate the DDPDA is meant to simulate how forecasters might use the algorithm if they were to issue a severe thunderstorm warning each time the DDPDA issued a downburst prediction. This does not take into account how forecasters might interpret the DDPDA output, or whether they would use the output, but is a simple comparison meant to be intuitively interpreted. The following is a brief overview of the evaluation criteria:

- Each cell in the database can be classified as a “hit,” “miss,” “false alarm,” or “correct null.”
- A hit occurs if one or more downburst predictions is issued for a cell up to four volume scans before the cell produces a downburst, plus the volume scan in which a downburst was observed.
- A miss occurs if a downburst prediction is not issued for a cell that produced a downburst.
- A false alarm occurs if one or more downburst predictions is issued for a cell that did not produce a downburst.
- A correct null occurs if the DDPDA issues no warnings and no downburst event occurs for a particular storm.
- Lead time is calculated with the assumption that a downburst prediction is issued at the end of a volume scan, rather than at the beginning, since DDPDA output becomes available only after the entire volume scan has been processed. Given the short-lived nature of the storm cells in the database, the maximum lead time is 15 min.

Although this method of scoring the DDPDA is fairly intuitive, there are still some potential weaknesses. This scoring technique does not reward multiple correct predictions or detections on long-lived downburst events. Additionally, although every effort is made to insure that the verification data are the best available, errors are inevitable because of the nature of how data are collected and used in *Storm Data*.

Heidke’s skill score [HSS; see Wilks (1995) for a discussion of various skill score calculations], along with probability of detection (POD), false alarm rate (FAR), and critical success index (CSI) are calculated for all 100 evaluation datasets in both range bands. HSS is the primary tool used to evaluate the skill of the algorithm, as it takes into account correct predictions of nonevents (null events) as well as correct forecasts. An HSS of 1.0 is equivalent to perfect forecast skill, while an HSS of 0 equates to the skill of results from purely random forecasts.

### 3. Results

The DDPDA has much better skill in the 20–45-km range, with a median HSS of 0.4, than in the 45–80-km range, with a median HSS of 0.17 (Fig. 3). This is

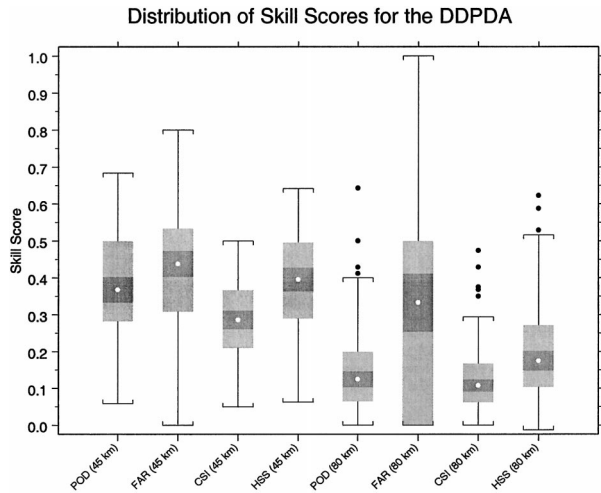


FIG. 3. Distribution of validation dataset skill scores for the 20–45-km (“45 km”) and 45–80-km (“80 km”) range bands. Each box-and-whisker chart shows the median value (white dot), 95% confidence interval of the median (dark gray box), interquartile range (IQR; light gray box),  $1.5 \times$  IQR (whiskers), and individual outliers (black dots) for 100 downburst prediction equations in each range band.

likely caused by poor beam resolution at long ranges and may be an artifact of a smaller sample size in the developmental dataset in the 45–80-km range band. Although the HSS at 45–80 km is about half that of the 20–45-km range band, the lower bound of the 95% confidence interval for the median is greater than zero, indicating that the prediction equations have skill. Additionally, the median lead time (Fig. 4) for the 20–45-km range is 5.5 min from the downburst prediction to the initial onset of outflow at the surface, while the median lead time for the 45–80-km range band is 0 min.

Figures 5 and 6 show the distributions of discriminant weights for all the variables, based on 100 prediction

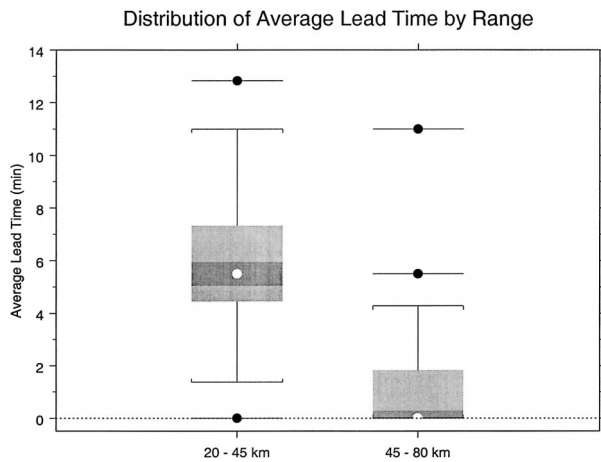


FIG. 4. The distribution of the mean lead times (min) from the issuance of a DDPDA downburst prediction to the initial onset of damaging outflow. See Fig. 3 for a description of the box-and-whisker diagrams.

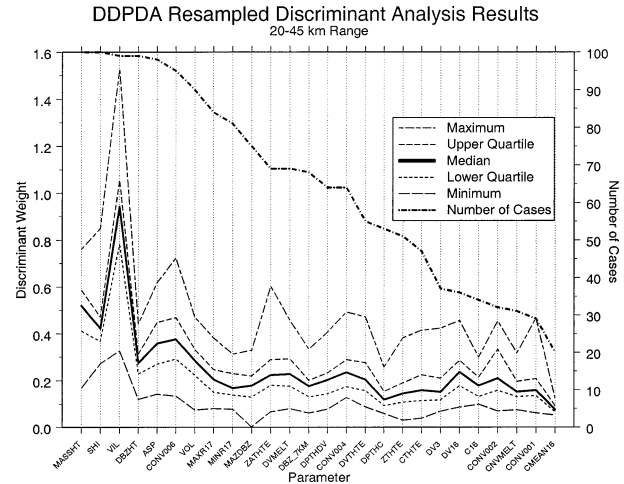


FIG. 5. The distribution of discriminant weights of each parameter for the 20–45-km range band and the number of DDPDA prediction equations (out of 100) in which they appeared. The parameters are described in Table 2.

equations, as well as the frequency with which each parameter appears in the equations. Discriminant analysis results exclude the variables that do not contribute to the discrimination between cells that produce downbursts and cells that do not. Therefore, when the dataset is resampled many times into new training and validation datasets, the most important parameters for detecting radar signatures that precede downburst events should appear in most of the corresponding prediction equations. Additionally, the mean discriminant weight (or standardized canonical coefficient) for each variable is given. This coefficient describes the relative contribution of each variable to the ability to discriminate between groups. The larger the standardized coefficient, the greater the contribution of that variable to the discrimination between downburst-producing storms and nondownburst storms.

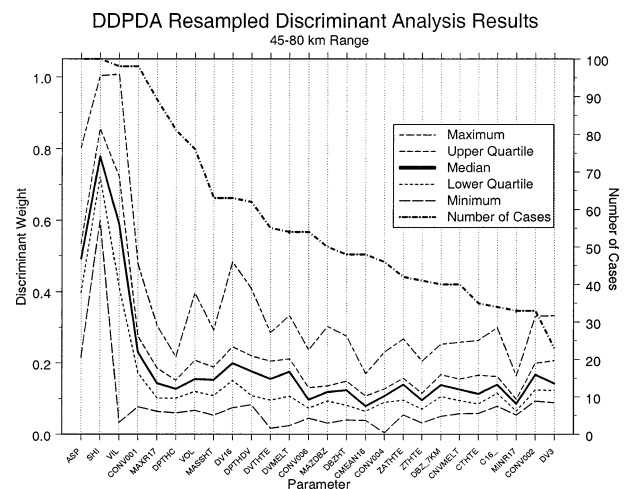


FIG. 6. Same as Fig. 5, except for the 45–80-km range band.

TABLE 3. The prediction equations based on the training datasets that produced the median HSS. The equations are of the form  $\mathbf{C}_1^T \mathbf{D} = D_1$  and  $\mathbf{C}_2^T \mathbf{D} = D_2$ , where  $\mathbf{C}_1$  and  $\mathbf{C}_2$  are column vectors of coefficients for the “nonsevere” and “severe” equations, respectively, and  $\mathbf{D}$  is the column vector of variables. A storm cell is classified as a potential severe downburst producer when  $D_2 > D_1$ . The variables are detailed in Table 2.

Range = 20–45 km			Range = 45–80 km		
$\mathbf{C}_1$	$\mathbf{C}_2$	$\mathbf{D}$	$\mathbf{C}_1$	$\mathbf{C}_2$	$\mathbf{D}$
−6.24503	−5.82639	VIL	0.1656	0.2764	SHI
0.08776	0.11501	SHI	152.5196	−298.7098	CTHTE
25.0406	23.3061	ASP	−3.4228	−3.1909	VIL
−118.9651	−38.4325	CONV006	12.6803	10.7156	ASP
463.5948	−8.0519	MAXR17	−1.1057	−1.2461	DPTHC
−7.0605	−5.8257	MASSHT	0.1654	0.1746	VOL
0.3164	0.2895	VOL	7.0397	6.9570	ZTHTE
10.5992	10.3789	MAXDBZ	1.1245	1.6754	MASSHT
573.705	275.8212	MINR17	−114.3302	−97.1857	CONV004
−1.6561	−2.0140	DBZHT	136.1785	398.0016	CMEAN16
586.3445	204.0834	CTHTE	−5.1821	−7.5902	CONV001
−52.6342	−59.5498	CONV002	0.7793	0.8424	DBZ_7KM
−3.1733	−3.0248	DPTHC	−0.1514	−0.2170	ZATHTE
3.6753	3.6099	ZTHTE	−824.2155	−566.4385	CNVMELT
−718.3489	−477.2294	CNVMELT	−2584.954	−2847.857	C16
1.4111	1.5052	DBZ_7KM	−4.6387	−4.8173	DBZHT
−0.9934	−1.08827	ZATHTE	−180.5065	−187.6453	1
−0.6446	−0.7164	DV3			
−356.9059	−353.2873	1			

Based on these weightings, the variables that appear to be most important to the timely prediction of downbursts in the 20–45-km range band include mostly reflectivity-based parameters: VIL, severe hail index (SHI), height of the center of mass (MASSHT), and core aspect ratio (ASP). The most important velocity-based variable is the cross-sectional area coverage of radial convergence exceeding  $0.006 \text{ s}^{-1}$  (CONV006). Several environmental parameters were also included in at least 50% of the equations but do not have a substantial impact in short-term predictions. This suggests that parameters that detect large, elongating reflectivity cores aloft are the most useful in downburst prediction at this range. It also suggests that the contribution of CONV006 as a convergence detection parameter strongly outweighs the contributions of most of the other radial velocity-based parameters, which are clustered with the other seldom-used variables near the far right of the graph.

The variables most important in the 45–80-km range band are the reflectivity-based SHI, VIL, and ASP parameters. Other variables that occurred frequently, but were not weighted as heavily, include the cross-sectional area coverage of radial convergence exceeding  $0.001 \text{ s}^{-1}$  (CONV001), the maximum rotational shear between 1 and 7 km mean sea level (MSL) (MAXR17), the depth of convergence exceeding  $0.004 \text{ s}^{-1}$  (DPTHC), and storm cell volume (VOL). The high weightings of the reflectivity-based parameters suggest most storms that produce strong outflows in this dataset likely include melting ice that causes cooling aloft and drives the downdrafts (Proctor 1989). The next three most-used parameters are all radial velocity-based variables that measure different aspects of the velocity field (conver-

gence strength and depth, rotation). However, the weighting of these variables in the discriminant equations are relatively low. The poor sampling of the velocity field at long ranges causes the radial convergence field to be weak and noisy; therefore, reflectivity-based indicators have the greatest contribution to discrimination between event types at these ranges.

The median HSS for each range band is a good estimator of the optimal expected long-term performance of each prediction equation. Therefore, the equations that give the median scores at each of the two range bands were chosen for inclusion in the DDPDA (Table 3). These median-performance equations are chosen rather than the equations that produced the best skill scores, because the “best” HSS scores are an artifact of the sampling of the training and validation datasets. There are two classifications equations for each range band. The equations  $\mathbf{C}_1^T \mathbf{D} = D_1$  and  $\mathbf{C}_2^T \mathbf{D} = D_2$  are solved for each storm cell, using coefficients  $\mathbf{C}_1$  and  $\mathbf{C}_2$  and the variable  $\mathbf{D}$  from Table 3. If  $D_2 > D_1$ , then the DDPDA issues a downburst prediction alert. If  $D_2 \leq D_1$ , then no alert is issued for the cell.

The median of the mean lead times (Fig. 4) for the 20–45-km range is 5.5 min from the downburst prediction to the initial onset of outflow at the surface, while the median of the mean lead times for the 45–80-km range band is 0 min. These relatively short lead times are not surprising given the nature of the environment. Individual storm cells that develop in an environment of weak vertical wind shear and moderate CAPE are usually short lived. In the downburst-producing storm cells used to develop the DDPDA’s prediction equations, the typical time from “first echo” aloft to the initial radar-detected outflow was 15 min.

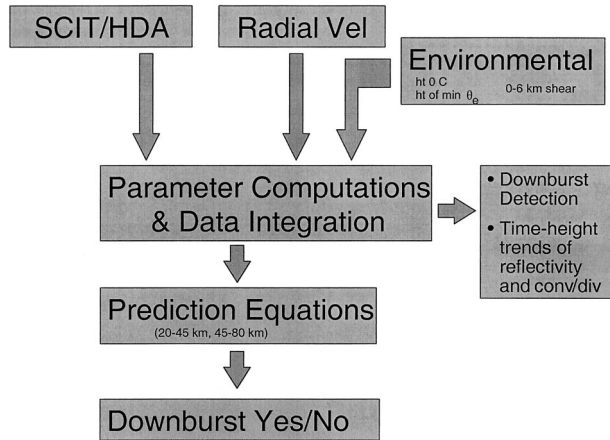


FIG. 7. An overview of DDPDA data flow.

However, most of the radar signatures that typically precede outflows may not be detected early in a storm cell's life cycle. Because the WSR-88D implements 5- or 6-min volume coverage patterns for detecting precipitation, temporal sampling may preclude timely detection of radar signatures. Lead times are calculated from the issuance of a downburst prediction at the end of a volume scan to the initial detection of outflow. Hence, locations at a distance from the initial outflow at the surface will have a longer lead time. Since Fig. 4 describes the median of mean lead times for each of the 100 sample validation datasets, many of the storm cells in the dataset had longer lead times than the median value. Additional usefulness may be derived from the DDPDA by using it in conjunction with environmental data to raise forecaster awareness that if downbursts have begun to occur, then nearby areas with similar environmental conditions should be closely monitored for new convection that may also produce strong outflows.

Finally, these results are biased by population density and the quality of spotter networks. Because most of the radars in our study are near major population centers, most of the population lies within 45 km of the radar, and the 45–80-km range band is not proportionally represented. The ratio of downburst events to nonevents in Table 1 is approximately 1:10 for the 20–45-km range band, while it is 1:18 in the 45–80-km range. While artifacts from the SCIT algorithm are partly responsible for these disproportional ratios, it is also likely that some storm cells classified as nonevents in the development dataset produced storm outflows that were counted as missed events in the DDPDA evaluation.

#### 4. Algorithm functional overview

A summary of the DDPDA functionality is shown in Fig. 7. The DDPDA receives input at the end of each volume scan from the SCIT algorithm, the HDA, and dealiased radial velocity data. The radial velocity field is processed as described above, and the parameters in

Table 2 are calculated for each storm cell. The DDPDA uses one of the discriminant functions detailed above (Table 3) to issue a “yes/no” downburst prediction for each cell, which can be displayed as an icon or in tabular format (Fig. 8a).

The DDPDA also provides information to users about ongoing downburst events. First, if a downburst has been detected via a low-level divergence signature that contains a radial wind exceeding  $25 \text{ m s}^{-1}$  or a velocity difference along a radial exceeding  $40 \text{ m s}^{-1}$ , then a “severe” downburst detection is issued by the DDPDA for that cell (Fig. 8b). Similarly, if a downburst has been detected via a low-level divergence signature that contains a radial wind exceeding  $18 \text{ m s}^{-1}$  or a velocity difference along a radial exceeding  $25 \text{ m s}^{-1}$ , then a “moderate” downburst detection is issued for the storm cell. This moderate downburst detection is intended for aviation use, as it is mainly a threat to aircraft in the takeoff/landing zone.

Finally, the DDPDA provides storm structure information to forecasters. This information comes in the form of time–height trends of reflectivity and convergence/divergence information (Fig. 8c). Such information can be helpful in assessing changes in storm intensity even for cases when the DDPDA does not issue predictions. These may also be useful in assessing the performance of the SCIT algorithm's identification techniques. For instance, poor SCIT algorithm performance will typically show cells that are discontinuous in the vertical, which may alert forecasters that the quantitative storm information produced by the SCIT algorithm (e.g., VIL) should not be trusted.

## 5. Discussion

### a. Operational implications

The primary users of the DDPDA are expected to be operational meteorologists and may also include aviation users. The National Weather Service has traditionally issued severe thunderstorm warnings for storms that produce winds in excess of  $26 \text{ m s}^{-1}$  (50 kt). However, downburst events that occur in an environment of weak vertical wind shear pose an extremely difficult challenge. In the dataset used to develop the DDPDA's downburst prediction equations, the typical amount of time between the first detection of a reflectivity core aloft and the low-altitude divergence signature indicating the onset of outflow is about 15 min, while the time between the first radar-detectable precursors to the outflow signature is frequently less than 10 min. Therefore, any automated guidance that can be provided to forecasters should be of great assistance. Downburst warnings by the DDPDA may help alert forecasters that downbursts have begun to occur. Frequently, an environment capable of producing one strong downburst will sustain more, until the boundary layer is stabilized by low equivalent potential temperature ( $\theta_e$ ) air. Thus, if

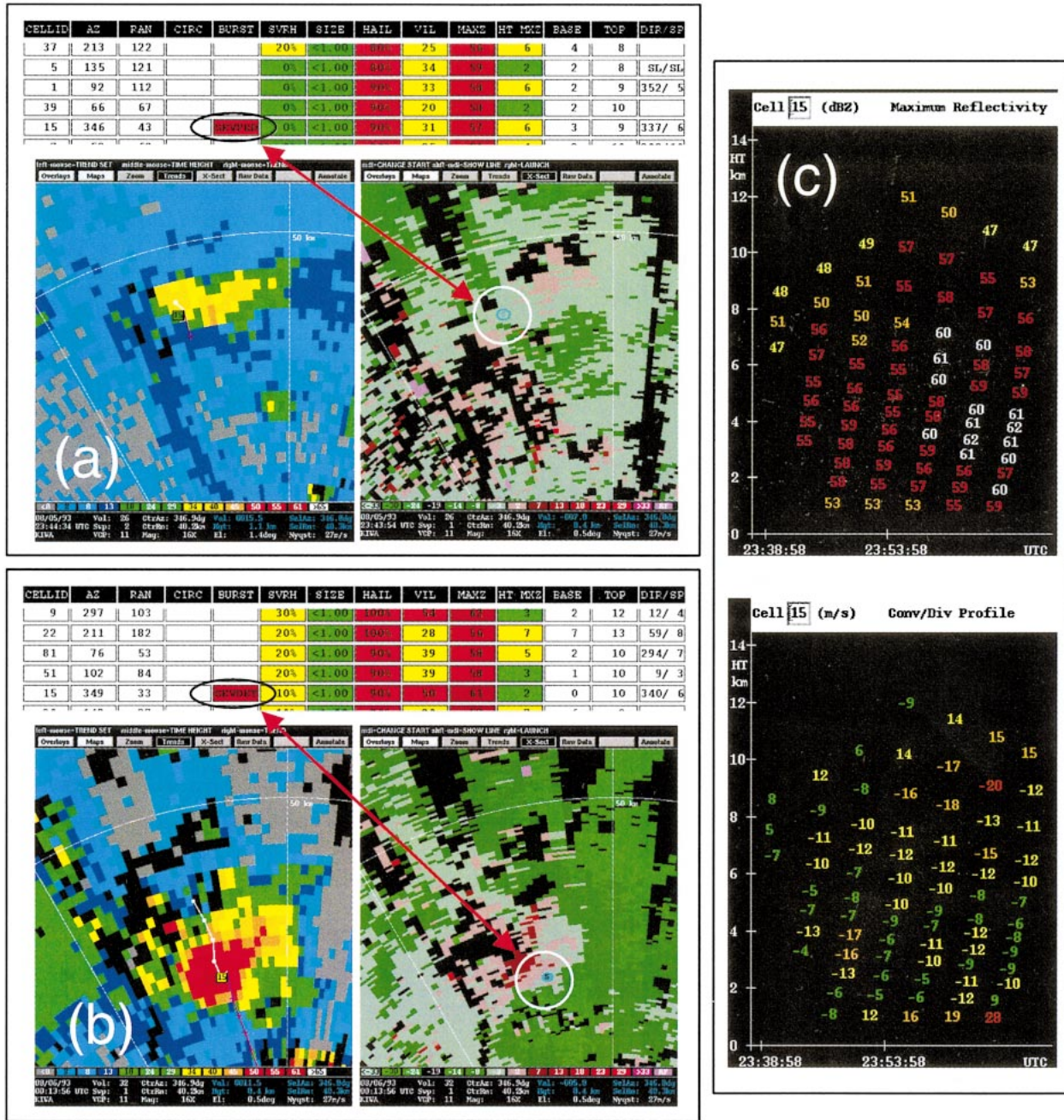


FIG. 8. (a), (b) Output of the DDPDA shown in National Severe Storms Lab's Warning Decision Support System (Eilts et al. 1996b). In (a), the SVRPRD label in the BURST column of the table indicates a severe downburst prediction for cell 15, while the oval "S" icon overlaid on radial velocity data indicates the same. In (b), the SVRDET label in the BURST column of the table and the filled-in oval "S" icon overlaid on the 0.5° radial velocity data indicate an ongoing severe downburst detection for the same cell 30 min later. (c) Time–height trends of (top) maximum reflectivity and (bottom) radial velocity difference for this cell. For radial velocity difference, positive values indicate radial divergence, while negative values indicate radial convergence.

one downburst has occurred, more will likely occur in the same area, as new cells develop along old outflows. Forecasters can use this knowledge to anticipate the development of severe storm cells.

The DDPDA is also useful as a wind shear alert tool for aviation users. Although most major airports in the

United States have some sort of wind shear alert system provided by a TDWR or Low Level Wind Shear Alert System, there are a significant number of general aviation airports that have no wind shear warning system in place. An examination of 1999 data from the U.S. Bureau of Transportation Statistics indicates that 3256

airports do not have any radar-based tools to help warn incoming or outgoing flights of dangers from wind shear. Of these, 1233 are within 80 km of a WSR-88D, implying that these airports could benefit from the addition of the DDPDA to the WSR-88D system.

### *b. Limitations and future work*

While the DDPDA shows skill in predicting downbursts in weakly sheared environments, the algorithm has not been designed to work in highly sheared environments. The vertical gradient of perturbation pressure can become a significant factor for downdrafts in supercell thunderstorms and mesoscale convective systems (Wakimoto 2001) and was not taken into consideration during the development of the DDPDA. Despite this, some intermediate DDPDA output, such as time-height trends of reflectivity and convergence for each cell, may still prove useful to forecasters in assessing storm structure.

Another weakness of the algorithm is its dependence on the SCIT algorithm, which frequently fails to correctly analyze quantitative storm parameters. Failures in the SCIT algorithm's storm tracking routines prohibit time derivatives of storm parameters from being used in the DDPDA prediction equations, which may limit the algorithm's performance. Some of the precursor signals to outflows that rely on temporal information cannot be fully assessed. Using an improved storm analysis and tracking routine may address this problem, allowing temporal derivatives of storm parameters to be easily added to the discriminant analysis classification functions.

More data are certainly needed to improve the quality and stability of the prediction equations generated with the linear discriminant analysis. The present prediction equations are based on data from low-shear environments that may be thermodynamically varied (e.g., subtropical versus desert). However, an expanded dataset may help development of equations that are more suited to a particular environment, thus improving the overall skill of the DDPDA.

The lead time of the DDPDA may be improved if the algorithm issues predictions as soon as a storm cell has been identified and scanned through a substantial depth, rather than at the end of a volume scan. This functionality has been designed into future versions of the SCIT algorithm (Wyatt 1998) and therefore should be fairly straightforward to implement in the DDPDA.

## **6. Conclusions**

This paper describes the Damaging Downburst Prediction and Detection Algorithm developed for use in the WSR-88D system. Although the resolution of data is somewhat coarser than in previous studies that have examined the evolution of downburst events produced by a single storm cell, a linear combination of derived

parameters can be used to predict whether or not a cell may produce a strong downburst. No single derived parameter is useful as a predictor by itself, as individual storm parameters did not discriminate well between cells that produced strong outflows and those that did not.

The DDPDA may provide a timely alert to forecasters and aviation users about impending strong outflows. The DDPDA predicts the occurrence of damaging winds at ranges where the middle and upper altitude of storm cells are well sampled by radar. At 20–45-km range, the DDPDA has an HSS of 0.40 and a median lead time of 5.5 min. At the longer 45–80-km range, the DDPDA has an HSS of 0.17 with a median lead time of 0 min. The short lead times are not surprising: Srivastava (1985) has shown that the time scale from downdraft formation to surface outflow is approximately 10 min. Since WSR-88D volume scans typically take 5–6 min between updates, it is not likely that the 5.5-min lead time shown by the DDPDA in the 20–45-km range can be significantly increased. Even downburst predictions with no lead time are useful, however, as they may help increase forecasters' awareness that other events are probable in a particular environment. The DDPDA does not issue downburst prediction warnings at longer ranges, where radar sampling has coarser resolution and the beam height is usually well above the outflow, making verification difficult. Downburst predictions are also not issued at ranges less than 20 km from the radar, as the WSR-88D only samples the lower levels of storms at these ranges.

The DDPDA also issues downburst detection warnings when strong convective winds are detected near the surface. However, the ability of the DDPDA to detect these strong outflows is largely dependent on the depth of the outflow. Shallow outflows at longer ranges may be only partially sampled or not sampled at all by the radar; thus, no detection warning will be issued in those instances.

There are several potentially beneficial modifications that could be made to this implementation of the DDPDA. In regions where coverage from multiple radars, including non-WSR-88Ds, overlaps significantly, it may be possible to take advantage of the better time resolution or to fill in gaps in the volume sampled by one radar with data from another. Additionally, we used a symmetric 5° azimuth by 5-km range gate kernel for the linear least squares velocity derivative estimates used in calculating convergence aloft. These derivative estimates could be made more accurate by use of an asymmetric kernel that varies in size with range. In regions where surface observations are dense, the DDPDA should make better use of the near-storm environment data to determine how potentially unstable the environment is to downdrafts. In this study, nearly all cases are from desert and subtropical climates that are thermodynamically different from each other, while plains and High Plains cases are conspicuously absent. The quality

of the available verification data dictates which regions receive the most attention, and although there have been many field experiments conducted in these regions, most of them predate the WSR-88D system. However, the algorithm may be easily tuned and tested in the future to accommodate the prevailing environmental conditions in a region, with an improvement in skill scores likely over the more environmentally generic classification equation presented in Table 3. It is important that the DDPDA be rigorously tested in all regions where strong downbursts occur before its implementation in the national WSR-88D system. Although we chose linear discriminant analysis to discriminate between severe and nonsevere cells, a nonlinear discriminant analysis could be employed to find nonlinear relationships between variables. Despite these issues, the DDPDA is the first successful tool to classify storm cells into severe and nonsevere wind producers developed specifically for the WSR-88D. As such, it represents a significant step forward by providing guidance about a difficult-to-anticipate phenomenon to operational forecasters.

*Acknowledgments.* This research is in response to requirements and funding by the Federal Aviation Administration (FAA). The views expressed are those of the authors and do not necessarily represent the official policy or position of the FAA. The Radar Operations center and the National Aeronautics and Space Administration provided additional funding. Other funding for this research was provided under NOAA–OU Cooperative Agreement NA17RJ1227. The authors wish to thank Kevin Scharfenberg and Jason Lynn for their early data collection efforts for this work. An early implementation of the DDPDA was conceived and designed by Mike Eilts, J. T. Johnson, DeWayne Mitchell, and Phillip Spencer (Eilts et al. 1996a). Thanks to Dr. Robert Maddox and the anonymous reviewers for their excellent feedback that helped improve this manuscript.

#### REFERENCES

- Atkins, N. T., and R. M. Wakimoto, 1991: Wet microburst activity over the southeastern United States. *Wea. Forecasting*, **6**, 470–482.
- Crum, T. D., and R. L. Alberty, 1993: The WSR-88D and the WSR-88D Operational Support Facility. *Bull. Amer. Meteor. Soc.*, **74**, 1669–1687.
- Eilts, M. D., J. T. Johnson, E. D. Mitchell, R. J. Lynn, P. Spencer, S. Cobb, and T. M. Smith, 1996a: Damaging Downburst Prediction and Detection Algorithm for the WSR-88D. Preprints, *18th Conf. on Severe Local Storms*, San Francisco, CA, Amer. Meteor. Soc., 541–545.
- , and Coauthors, 1996b: Severe weather warning decision support system. Preprints, *18th Conf. on Severe Local Storms*, San Francisco, CA, Amer. Meteor. Soc., 536–540.
- Elmore, K. M., E. D. Albo, R. K. Goodrich, and D. J. Peters, 1994: NASA/NCAR airborne and ground-based wind shear studies. Final Report, Contract NCC1-155, 343 pp.
- Federal Aviation Administration, 1987: *Windshear Training Aid*. 4 Vols. Washington, DC, 344 pp.
- Fujita, T. T., 1981: Tornadoes and downbursts in the context of generalized planetary scales. *J. Atmos. Sci.*, **38**, 1511–1534.
- Hjelmfelt, M. R., 1988: Structure and life cycle of microburst outflows observed in Colorado. *J. Appl. Meteor.*, **27**, 900–927.
- Huberty, C. J., 1994: *Applied Discriminant Analysis*. John Wiley and Sons, 466 pp.
- Johns, R. H., and W. D. Hirt, 1987: Derechos: Widespread convectively induced windstorms. *Wea. Forecasting*, **2**, 32–49.
- Johnson, J. T., P. L. MacKeen, A. Witt, E. D. Mitchell, G. J. Stumpf, M. D. Eilts, and K. W. Thomas, 1998: The Storm Cell Identification and Tracking algorithm: An enhanced WSR-88D algorithm. *Wea. Forecasting*, **13**, 263–276.
- Klazura, G. E., and D. A. Imy, 1993: A description of the initial set of analysis products available from the NEXRAD WSR-88D system. *Bull. Amer. Meteor. Soc.*, **74**, 1293–1311.
- Mahoney, W. P., and K. L. Elmore, 1991: The evolution and fine-scale structure of a microburst-producing cell. *Mon. Wea. Rev.*, **119**, 176–192.
- Mitchell, E. D., S. V. Vasiloff, G. J. Stumpf, A. Witt, M. D. Eilts, J. T. Johnson, and K. W. Thomas, 1998: The National Severe Storms Laboratory Tornado Detection Algorithm. *Wea. Forecasting*, **13**, 352–366.
- Proctor, F. H., 1989: Numerical simulations of an isolated microburst. Part II: Sensitivity experiments. *J. Atmos. Sci.*, **46**, 2143–2165.
- Roberts, R. D., and J. W. Wilson, 1989: A proposed microburst nowcasting procedure using single-Doppler radar. *J. Appl. Meteor.*, **28**, 285–303.
- Srivastava, R. C., 1985: A simple model of evaporatively driven downdraft: Application to microburst downdraft. *J. Atmos. Sci.*, **42**, 1004–1023.
- Stumpf, G. J., A. Witt, E. D. Mitchell, P. L. Spencer, J. T. Johnson, M. D. Eilts, K. W. Thomas, and D. W. Burgess, 1998: The National Severe Storms Laboratory Mesocyclone Detection Algorithm for the WSR-88D. *Wea. Forecasting*, **13**, 304–326.
- Wakimoto, R. M., 2001: Convectively driven high wind events. *Severe Convective Storms, Meteor. Monogr.*, No. 50, Amer. Meteor. Soc., 255–298.
- Wilks, D. S., 1995: *Statistical Methods in the Atmospheric Sciences*. Academic Press, 465 pp.
- Witt, A., M. D. Eilts, G. J. Stumpf, J. T. Johnson, E. D. Mitchell, and K. W. Thomas, 1998: An enhanced hail detection algorithm for the WSR-88D. *Wea. Forecasting*, **13**, 286–303.
- Wolfson, M. M., R. L. Delaney, B. E. Forman, R. G. Hallowell, M. L. Pawlak, and P. D. Smith, 1994: Automated microburst wind-shear prediction. *Lincoln Laboratory Journal*, Vol. 7, MIT, 399–426.
- Wyatt, A. L., E. D. Mitchell, G. J. Stumpf, and A. Witt, 1998: “Rapid update” of radar-derived severe weather algorithms. Preprints, *19th Conf. on Severe Local Storms*, Minneapolis, MN, Amer. Meteor. Soc., 788–789.